NRC·CNRC

NRC Publications Archive
Archives des publications du CNRC

Simulation of gas-substrate heat exchange during cold-gas dynamic spraying

Ryabinin, A. N.; Irissou, E.; McDonald, A.; Legoux, J.-G.

This publication could be one of several versions: author's original, accepted manuscript or the publisher's version. / La version de cette publication peut être l'une des suivantes : la version prépublication de l'auteur, la version acceptée du manuscrit ou la version de l'éditeur.
For the publisher's version, please access the DOI link below./ Pour consulter la version de l'éditeur, utilisez le lien DOI ci-dessous.

Publisher's version / Version de l'éditeur:
https://doi.org/10.1016/j.ijthermalsci.2012.01.007
International Journal of Thermal Sciences, 56, June, pp. 12-18, 2012-02-15

NRC Publications Record / Notice d'Archives des publications de CNRC:
https://nrc-publications.canada.ca/eng/view/object/?id=89916b10-5e8c-4fd4-9591-01ff72efb6b7
https://publications-cnrc.canada.ca/fra/voir/objet/?id=89916b10-5e8c-4fd4-9591-01ff72efb6b7

Access and use of this website and the material on it are subject to the Terms and Conditions set forth at
https://nrc-publications.canada.ca/eng/copyright
READ THESE TERMS AND CONDITIONS CAREFULLY BEFORE USING THIS WEBSITE.

L'accès à ce site Web et l'utilisation de son contenu sont assujettis aux conditions présentées dans le site
https://publications-cnrc.canada.ca/fra/droits
LISEZ CES CONDITIONS ATTENTIVEMENT AVANT D'UTILISER CE SITE WEB.

Questions? Contact the NRC Publications Archive team at PublicationsArchive-ArchivesPublications@nrc-cnrc.gc.ca. If you wish to email the authors directly, please see the first page of the publication for their contact information.

Vous avez des questions? Nous pouvons vous aider. Pour communiquer directement avec un auteur, consultez la première page de la revue dans laquelle son article a été publié afin de trouver ses coordonnées. Si vous n'arrivez pas à les repérer, communiquez avec nous à PublicationsArchive-ArchivesPublications@nrc-cnrc.gc.ca.

National Research Council Canada | Conseil national de recherches Canada

Canada

lick here to view linked References

Simulation of Gas-Substrate Heat Exchange during Cold Gas Dynamic Spraying

A.N. Ryabinin[a], E. Irissou[b], A. McDonald[c], J.-G. Legoux[b]

[a]*Institute of Mathematics and Mechanics*
St. Petersburg University, St. Petersburg, Russia

[b]*National Research Council Canada*
Industrial Materials Institute, Boucherville, Québec, J4B 6Y4, Canada

[c]*Department of Mechanical Engineering*
4-9 Mechanical Engineering Building
University of Alberta, Edmonton, Alberta, T6G 2G8, Canada
Telephone: +001(780)4922675
Fax: +001(780)4922200
Corresponding Author Email: andre.mcdonald@ualberta.ca

ABSTRACT

In this study, the Nusselt numbers of impinging compressible fluid jets originating from a cold-gas dynamic spraying nozzle were determined. A low-pressure cold-gas dynamic spraying unit was used to generate a jet of hot compressed nitrogen that impinged upon flat substrates. Computer codes based on a finite differences method were used to solve the governing 3-D temperature distribution equation for the substrate to produce a non-dimensional relationship between the Nusselt number and the radius of the impinging fluid jet. It was found that the Nusselt number decreased as the non-dimensional radius of the jet from the stagnation point increased. It was found further that for small values of the Biot number, a simplified 2-D approximation of the substrate temperature distribution produced substrate surface temperature profiles that were in close agreement with that which was determined from the more complex 3-D temperature distribution model.

Highlights

- Surface temperature under air jet in cold spraying
- Variation of Nusselt number with radius of spreading jet
- Agreement of 2-D and 3-D temperature distribution models

KEYWORDS

Biot number; Cold spraying; Jet impingement; Nusselt number; Temperature distribution

NOMENCLATURE

Bi	Biot number
c_p	specific heat (J/kg-°C)
D	cold spray nozzle diameter (m)
f	arbitrary function
Fo	Fourier number
g	arbitrary function
h	heat transfer coefficient (W/m^2-K)
H	substrate height (m)
k	thermal conductivity (W/m-K)
l	substrate thickness (m)
L	substrate length (m)
Nu	Nusselt number
q'''	volumetric energy generation (W/m^3)
r	radial coordinate
t	time (s)
T	temperature (°C)
V	nozzle velocity (m/s)
x	linear coordinate
y	linear coordinate

Greek Symbols

α	thermal diffusivity (m^2/s)
θ	non-dimensional temperature
ξ	non-dimensional radius
ρ	density (kg/m^3)

Subscripts

aw	adiabatic wall
g	gas
i	initial
s	substrate
sur	surface
∞	ambient

1. INTRODUCTION

Cold-gas dynamic spraying ("cold spraying") is a process in which small, un-melted metal or alloy powder particles (1 – 100 μm in diameter) are accelerated to high speeds (500 to 1200 m/s) by a supersonic gas flow to form a dense protective or functional coating [1]. This high speed impact promotes plastic deformation to form strong bonds within the coating. It has been shown extensively that parameters such as the propellant gas temperature [1 – 4] and particle in-flight velocity affect the adhesion of the particles during deposition to fabricate the coating [4 – 7]. To maximize particle speed, actual cold spray systems allow pre-heating of the nitrogen or helium propellant gas up to 1000°C [8]. Therefore, significant substrate surface heating is expected upon impact of this pre-heated supersonic gas stream.

Recent studies have focused attention on the impact of the substrate surface temperature on the deposition behavior of cold-sprayed metals and on the fabrication of the coatings. Fukumoto, *et al.* [9], through fundamental analysis of individual particles, have shown that increasing the temperature of mirror-polished stainless steel and aluminum substrates will increase the deposition rate of cold-sprayed copper particles. Further work by Legoux, *et al.* [10], which focused on the effects of surface temperature variation on the microstructure of macroscopic aluminum and tin coatings, showed that increasing the substrate surface temperature increased the particle deformation within the coating and the coating-substrate contact. The aforementioned studies have led other investigators to investigate and combine surface heating with cold spray deposition to improve the overall quality of the final coatings. Kulmala and Vuoristo [11], Danlos, *et al.* [12], and Lupoi *et al.* [13] have combined cold spraying with laser-assisted surface heating to improve coating deposition efficiency, density, and adhesion strength

of copper-alumina, nickel-alumina, and aluminum coatings onto either steel or aluminum 2017 alloy substrates. Other investigators [14] have shown that material properties of the substrate such as thermal conductivity will impact the substrate surface temperature, contributing to the generation of residual stresses in the final coating. The effects of modifying the substrate surface temperature have been improvements in the overall microstructural quality of the final coatings and management of heat transfer to temperature sensitive substrate materials. However, with the exception of a few studies [15], widespread analyses of the fundamental heat transfer between the cold spray compressed gas jet and the substrate surface still needs to be explored.

Compressed gas jet impingement heat transfer is the dominant mode of energy exchange between the cold spray system and the substrate. Numerous analytical, numerical, and experimental investigations have been conducted to study the heat transfer from compressible gas jets to flat surfaces and quantify the heat transfer coefficients or Nusselt numbers [15 – 21]. Early work by Belov, *et al.* [16] focused on mathematical modeling of the heat transfer and heat flux between a supersonic under-expanded jet and a flat plate. It was suggested that the complex turbulence flow pattern of the impinging jet resulted in deviations between the experimental measurements and the predictions of the analytical model. Research focus has been aimed at quantification of the Nusselt number of compressible gas jet impingement flow. Rahimi, *et al.* [18] has shown that the Nusselt number for the impingement of compressed under-expanded supersonic air jets onto heated flat steel substrates may be as high as 1700. Lee, *et al.* [17] coupled the results of a one-dimensional transient heat conduction model of the substrate with experimental data to estimate the Nusselt number. The heat transfer coefficient and Nusselt number appeared in a boundary condition and in the expression for the eigenvalues during

solution of the governing partial differential equation of the model. It was found further that the maximum heat transfer coefficients and heat flux occurred at the stagnation point of the jet [15, 17 – 19]. While these studies establish strong fundamental concepts in the area of heat transfer during jet impingement, specific studies are required that focus attention on the cold spraying process where the jet will be in axial motion.

The cold spraying process is one in which solid particles, loaded into the gas jet, are deposited on the surfaces. A study by Yoshida, *et al.* [22] has shown that around the stagnation point of air jets containing spherical glass beads during impact on a flat plate, the Nusselt number was approximately 2.7 times greater than that found in single-phase air impingement flow studies. The increase in the Nusselt number was attributed to the disturbance of the flow and thermal fields at the solid surface by the spherical particles. Yokomine, *et al.* [23] extended the work of Yoshida, *et al.* [22] to show that the type and size of the solid particles in the jet could either decrease or increase the Nusselt number found in single-phase air impingement flow studies. The inclusion of small graphite particles into the air jet enhanced heat transfer, while the inclusion of large glass beads reduced the heat transfer.

The present study examines the heat transfer between stationary and axially moving cold spraying nozzles that are used to generate heated, compressed air jets. Through the use of experimentation and numerical simulation, the Nusselt number as a function of the radius of the spreading jet on the substrate surface after impingement is determined. The surface temperature distribution of a variety of substrates is used to validate the model and the results for Nusselt number.

2. EXPERIMENTAL AND NUMERICAL METHODS

A low-pressure cold-gas dynamic spraying system (SST Series P, Centerline, Ltd., Windsor, ON, Canada) was used to generate a jet of hot compressed nitrogen. The pressure and temperature of the nitrogen gas were 690 kPa (100 psig) and 100 – 200°C, respectively at the cold spray system console. The converging-diverging de Laval nozzle in the cold spray torch was 140 mm long, had a throat diameter of 2.54 mm, and an exit diameter of 6.3 mm. During operation, the cold spray nozzle was manipulated by a robot (Motoman-HP20, Yaskawa Electric Corporation, Waukegan, IL, USA). The stand-off distance, the distance between the nozzle and the substrate, was fixed at 10 mm. For stationary nozzle tests, the nozzle was moved from the outside to the middle of the substrate at a speed of 1 m/s. For moving nozzle tests, the nozzle was moved across the substrate to scan a line at the center of the substrate at a transverse speed of 10 mm/s.

The substrates were mounted on a substrate holder and with a thermo-insulator material (Alumina Insulation Type SALI Al_2O_3-SiO_2, ZIRCAR , Florida, NY, USA) placed between them. The insulation was used to restrict the heat exchange between the ambient air and the substrate surface only. A blower was used to create airflow of approximately 3.8 m^3/s, ensuring a constant ambient room temperature for heat exchange in proximity to the substrate. A variety of substrate materials, prepared in square geometries, were considered. Copper, steel 1020, steel 430, and Lexan (SABIC Innovative Plastics, Pittsfield, MA, USA) were used. Lexan is a polycarbonate resin thermoplastic with low thermal conductivity (0.2 W/m-K). Most of the substrates had a square dimension of 76.2 mm. For tests that involved the stationary cold spray nozzle, the nitrogen gas jet impinged the center of the substrate.

Steady-state temperature measurements of the surface of the substrates were taken by using an infrared camera (ThermaCAM SC-Series 3000, FLIR Systems, Sweden). The camera had a spatial resolution of 0.6 mm, a spectral range of 8 to 9 mm, and a time resolution of 17 ms. In order to approach ideal black-body radiation, the substrate surface was painted black with a high-temperature paint that has an emissivity of 0.95.

Computer codes based on a finite differences method were generated to solve the governing temperature equations and determine the heat transfer coefficient of the impinging compressible fluid jet. A Runge-Kutta fourth-order method was employed by the time solver. The codes were written in Pascal and the maximum number of grid points was 11,000. The heat transfer coefficient obtained was also used in the heat transfer calculations for the case of the moving cold spray nozzle. For these calculations, the dimensionless time step parameter, $\frac{V\Delta t}{\Delta x}$, was less than 1.

3. MATHEMATICAL MODEL

The impingement of a hot supersonic gas jet on to a solid surface will result in rapid surface heating near the impingement or stagnation point of the jet. Estimation of the heat transfer coefficient (h) of the spreading gas film, which is directly proportional to the heat transfer rate from the gas to the solid surface, will need to be conducted. Figure 1 shows a schematic of the model used in the analysis. In this study, the supersonic jet impacts upon the surface to spread axisymmetrically as a thin gas film on the solid surface at $z = l$ (see Fig. 1). All other sides of the

solid substrate were modeled as being insulated. The thickness of the substrate ($0 < z < l$) was much smaller than the length ($0 < x < L$) and height ($0 < y < H$).

The governing equation of the general 3-D temperature distribution in the substrate is

$$\frac{k_s}{\rho_s c_{ps}}\left(\frac{\partial^2 T}{\partial x^2}+\frac{\partial^2 T}{\partial y^2}+\frac{\partial^2 T}{\partial z^2}\right)=\frac{\partial T}{\partial t}. \tag{1}$$

The boundary conditions and initial condition are

$$\frac{\partial T(0,y,z,t)}{\partial x}=0, \tag{2}$$

$$\frac{\partial T(L,y,z,t)}{\partial x}=0, \tag{3}$$

$$\frac{\partial T(x,0,z,t)}{\partial y}=0, \tag{4}$$

$$\frac{\partial T(x,H,z,t)}{\partial y}=0, \tag{5}$$

$$\frac{\partial T(x,y,0,t)}{\partial z}=0, \tag{6}$$

$$\frac{\partial T(x,y,l,t)}{\partial z}=\frac{h}{k_s}[T_{aw}-T(x,y,l,t)], \tag{7}$$

$$T(x,y,z,0)=T_i. \tag{8}$$

A substrate with a rectangular geometry that possesses a small thickness will experience a small temperature variation through the cross section of the thickness. The criterion for assuming negligible temperature variation at a given cross section is that the Biot number is small compared to unity [24]. The Biot number is the ratio of the internal conduction and external convection resistances and is

$$\mathrm{Bi} = \frac{hl}{k_s}. \tag{9}$$

In this case, the substrate temperature distribution may be approximated as being two-dimensional, and simple averaging across the thickness of the substrate may be used. The z-component conduction term in Eq. 1 may be rewritten as

$$\frac{\partial^2 T}{\partial z^2} = \frac{\partial\left(\frac{\partial T}{\partial z}\right)}{\partial z} \approx \frac{\frac{\partial T(x,y,l,t)}{\partial z} - \frac{\partial T(x,y,0,t)}{\partial z}}{l} = \frac{h}{k_s l}\left[T_{\mathrm{aw}} - T(x,y,l,t)\right]. \tag{10}$$

Eq. 10 can be substituted into Eq. 1 to give a 2-D governing equation for the approximate substrate temperature distribution as

$$\frac{1}{\rho_s c_{\mathrm{ps}} l}\left[k_s l\left(\frac{\partial^2 T}{\partial x^2} + \frac{\partial^2 T}{\partial y^2}\right) + h\left[T_{\mathrm{aw}} - T(x,y,l,t)\right]\right] = \frac{\partial T}{\partial t}. \tag{11}$$

The boundary conditions of Eqs. 2 – 5 and the initial condition of Eq. 8 were used in the solution of Eq. 11. In Eqs. 1 and 11, the heat transfer coefficient of the impinging gas is an unknown parameter that needs to be determined. For the case of slender substrates, that is, substrates

where the length and width are much larger than the thickness, the results of the approximate 2-D heat conduction model (Eq. 11) will be compared to those of the general 3-D model (Eq. 1). For non-slender substrates, only the 3-D conduction model will apply.

It is typical to express the heat transfer coefficient as a non-dimensional Nusselt number, defined as

$$\mathrm{Nu} = \frac{hD}{k_g}. \tag{12}$$

Eqs. 1 and 11 suggests that the heat transfer coefficient will vary in spatial coordinates. The schematic of Fig. 1 shows that the gas film will spread radially over the surface of the substrate. Therefore, it is expected that the heat transfer coefficient will vary radially from the stagnation point of the impinging gas jet. So, $h = f(r)$ and $\mathrm{Nu} = g(r)$.

The adiabatic wall temperature (T_{aw}) shown in Eqs. 7 and 11 will need to be determined. Computational fluid dynamics (CFD) method for adiabatic wall temperature determination is associated with the involvement of complex mathematical models and requires significant computational resources. To alleviate these difficulties, an infrared camera was used to measure the radial surface temperature of a Lexan plate (low thermal conductivity material) under the gas film. These temperatures were measured after steady-state and equilibrium was established, and represented approximate values of the radial adiabatic wall temperature under the spreading, compressed hot gas film. With known values of the adiabatic wall temperature, Eqs. 1 and 11 were applied to a variety of metal substrates to estimate and verify the spatially varying heat transfer coefficient of the spreading gas jet.

4. RESULTS AND DISCUSSION

The impingement of a cold spray gas jet upon a flat substrate surface will result in surface heating that may improve the deposition efficiency of the final coating [9, 10]. Modeling of the surface temperature of the substrate will prove useful in determining the optimum conditions for improved coating quality. However, knowledge of the heat transfer coefficient is necessary to estimate the surface temperature. The adiabatic wall temperature of the gas jet is required to estimate the heat transfer coefficient. Figure 2 shows the variation of the non-dimensional adiabatic wall temperature (θ) with non-dimensional radial distance (ξ) from the stagnation point of the jet on the surface of a low thermal conductivity Lexan substrate. By using a low thermal conductivity material, the amount of heat dissipated into the substrate will be constrained, and the surface temperature will approach the adiabatic wall temperature. The following variables were used to non-dimensionalize the adiabatic wall temperature and the radius of the spreading jet:

$$\theta_{aw} = \frac{T_{aw} - T_\infty}{T_g - T_\infty}, \quad \xi = \frac{r}{D}. \tag{13}$$

The temperature of the nitrogen gas that was measured at the cold spray console (T_g) was 100°C and the ambient temperature (T_∞) was 21°C. However, the use of a non-dimensional temperature will expand the applicability of Eq. 13 to other values of T_g. The figure shows that the adiabatic wall temperature of the surface under the spreading jet is a maximum at the stagnation point and decreases in the radial direction, away from the point. For an ideal adiabatic surface, the wall temperature would be the adiabatic wall temperature, which should be greater than the free stream temperature of the working fluid [25] at the jet stagnation point due to dissipation effects. However, Fig. 2 shows that at the stagnation point ($\xi = 0$), the non-dimensional adiabatic wall temperature is approximately 0.85, indicating that T_{aw} is less than T_g. This is likely due to a lower

temperature gas impacting the surface of the Lexan substrate. T_g is the gas temperature within the cold spray nozzle. Due to extensive mixing and heat exchange outside of the nozzle with the colder ambient air, the gas temperature is reduced. Work by Kosarev *et al.* [15] have shown further that the impingement of hot air jets in cold spraying onto heat conductive materials will produce substrate surface temperatures that are lower than the stagnation temperature due to conduction of heat into the material. This would be less likely for materials that possess low thermal conductivities.

Knowledge of the adiabatic wall temperature will permit numerical determination of the heat transfer coefficient and Nusselt number with Eqs. 11 and 12, after solution of either Eqs. 1 or 11. The surface temperature of a variety of substrates, $T(x,y,l,t)$, under the impinging and spreading jet was measured experimentally with an infrared camera and used in the numerical solutions of Eqs. 1 and 11. Figure 3 shows the Nusselt number (Nu) variation with non-dimensional radial distance from the stagnation point of the jet. The figure presents the results of the numerical finite difference method at various non-dimensional radii from the stagnation point. The points were fitted with a smooth curve function that is the sum of three Lorentzians. Similar to the variation of the adiabatic wall temperature presented in Fig. 2, the Nusselt number decreases as the radial distance from the jet stagnation point increases. Simple scaling analysis conducted by Jiji [26] have shown that the local Nusselt number for external laminar, incompressible flow over flat plates is directly proportional to the velocity of the fluid. Shapiro [25] has shown further that for laminar and turbulent flow of compressible gases, the Nusselt number varies proportionally with the square-root of the Reynolds number and the gas velocity. It is expected that as the jet spreads and flows away from the stagnation point, growth of the jet will retard the flow, reducing

the gas velocity [18]. This will result in a reduction of the Nusselt number as the radial distance from the stagnation point is increased. In general, a similar trend was observed by Rahimi, *et al.* [18].

The method of estimation of the Nusselt number variation of a gas from a stationary cold spray nozzle was simple and did not require complex derivations and calculations typical of compressible flow heat convection problems. In order to validate the Nusselt numbers presented in Fig. 3, the gas was sprayed upon a low carbon steel plate with the stationary cold spray nozzle. The surface temperature of the steel at the stagnation point of the jet was measured experimentally and calculated numerically, with the Nusselt number from Fig. 3, and with time as the independent variable. Figure 4 shows the transient variation of the non-dimensional surface temperature of the steel (θ_{sur}) at the jet stagnation point ($\xi = 0$). The non-dimensional time is the Fourier number (Fo), and it is

$$\mathrm{Fo} = \frac{\alpha_s t}{D^2} \ . \tag{14}$$

The figure shows that the non-dimensional temperature increases rapidly and achieves steady-state quickly. Due to the larger thermal conductivity of steel (approximately 60 W/m-K), more heat diffuses through the material than in the case of Lexan. Therefore, the steady-state non-dimensional temperature at the stagnation point of the jet is approximately 0.5, compared to 0.85 on Lexan (see Fig. 2). Both the experimentally measured and the numerically calculated temperatures are presented in Fig. 4. The numerical model results agree well with the experimentally measured transient temperature.

Further validation of the results presented in Fig. 3 for the Nusselt number can be obtained by studying the radial surface temperature distribution under the spreading jet for a variety of substrate materials. Figure 5 shows the non-dimensional surface temperature distribution of steel 430, steel 1020, and copper. To test the flexibility of the model and the application of the Nusselt number results of Fig. 3, substrate samples with square dimension of 76.2 mm and thickness of 3.1 mm were exposed to the gas jet via the stationary cold spray nozzle. One additional sample of steel 1020 was a square of dimension of 177.8 mm and thickness of 3.1 mm. It can be seen from Fig. 5 that the numerical model results of the surface temperature distributions of all the substrates agree well with the experimentally measured surface temperatures. In the case of the steel 1020 substrate with a square of dimension of 177.8 mm (Fig. 5b), the deviation between the experimental and numerical results increased with increasing radial distance from the stagnation point of the jet. This was probably due to errors induced by significant heat loss from the periphery of the square plate. This is confirmed by the lower values of the experimentally measured temperatures (see Fig. 5b). It has been observed in this study that on materials with larger thermal conductivity, the non-dimensional surface temperature at the stagnation point of the jet is lower (compare Figs. 2 and 4). This is further confirmed by analyzing Fig. 5, in which the non-dimensional surface temperature of the copper plate ($k_s \approx 400$ W/m-K) at the stagnation point is approximately 0.35, while that for the steel samples ($k_s \approx 60$ W/m-K) is approximately 0.55 to 0.70.

The Nusselt numbers presented in Fig. 3 can be used to validate the assumption of negligible temperature variation through the cross sections of substrates with low thicknesses, and that the

substrate temperature distribution was two-dimensional. With the heat transfer coefficient determined from Eq. 12 and Nusselt numbers from Fig. 3, the maximum Biot number (from Eq. 9) at the jet stagnation point on the steel and copper substrates are approximately 0.70 and 0.10, respectively. Beyond the stagnation point, the Biot number decreases significantly since the Nusselt number and heat transfer coefficient decrease. Since the Biot numbers are small compared to unity, the two dimensional assumption of the temperature distribution that governs Eq. 11 can be used to estimate the heat transfer coefficient on these surfaces. For substrates with larger thickness, the Biot number is on the order of unity or larger. So, the complete three-dimensional model (Eq. 1) would provide more accurate estimates of the heat transfer coefficient and the Nusselt number.

In the cold spraying deposition process to fabricate a coating, the nozzle traverses the substrate surface. It is expected that given the low traverse velocities typical of the cold spraying process (2 to 50 mm/s) [4, 10], variations of the heat transfer coefficient and Nusselt number developed under the stationary nozzle should be small. Figure 6 presents the non-dimensional surface temperature variation of a painted low-carbon steel substrate. Both experimental and numerical surface temperature distributions are shown. The paint on the surface of the steel was black and served to facilitate measurement of the temperature by the infrared camera. The nozzle velocity was 10 mm/s, and traversed the substrate linearly through the center of the steel plate. The asymmetric shape of the curves, coupled with higher temperatures in the negative non-dimensional radial direction, indicates that the nozzle was moved from right to left. While some deviations exist, the numerical estimate of the surface temperature distribution agrees well with the experimentally measured temperature distribution. The presence of a low thermal

conductivity black paint on the surface resulted in higher experimental temperatures compared to the numerically determined temperatures (see Fig. 6). The presence of the paint was not included in the numerical simulation of the surface temperature distribution, resulting in the deviations observed. For the stationary nozzle, steady-state was established. Therefore, these deviations were not observed.

5. CONCLUSION

The Nusselt numbers of impinging compressible fluid jets originating from a cold-gas dynamic spraying nozzle were determined through the use of a simplified governing heat conduction model and numerical analysis. It was found that the Nusselt number decreased as the non-dimensional radius of the jet from the stagnation point increased, which agrees with trends observed by other investigators. It was found further that for small values of the Biot number, a simplified 2-D approximation of the substrate temperature distribution produced substrate surface temperature profiles that were in close agreement with that which was determined from the more complex 3-D temperature distribution model.

In industrial practice, the compressed gas jet of the cold spraying process will include solid particles. These particles may have an impact on the Nusselt number and heat exchange between the two-phase jet flow and the substrate surface. Further study to determine the Nusselt number for cold spray gas jets containing solid particles will be required for broader understanding of the effect of substrate heating on particle deposition and coating quality.

6. ACKNOWLEDGEMENTS

The authors gratefully acknowledge the technical assistance of Mr. Frederic Belval.

7. REFERENCES

[1] A. Papyrin, V. Kosarev, K. Klinkov, A. Alkhimov, V. Fomin, Cold Spray Technology, Elsevier, Oxford, 2006.

[2] V. Champagne, The Cold Spray Materials Deposition Process: Fundamentals and Applications, Woodhead Publishing Limited, Cambridge, 2007.

[3] R. Maev, V. Leshchinsky, Introduction to Low Pressure Gas Dynamic Spray: Physics and Technology, Wiley-VCH Verlag GmbH, Weinheim, 2008.

[4] P. King, G. Bae, H. Zahiri, M. Jahedi, C. Lee, An experimental and finite element study of cold spray copper impact onto two aluminum substrates, J. Therm. Spray Technol. 19 (2010) 620-634.

[5] T. Stoltenhoff, H. Kreye, H. Richter, An analysis of the cold spray process and its coatings, J. Therm. Spray Technol. 11 (2002) 542-550.

[6] F. Gärtner, T. Stoltenhoff, T. Schmidt, H. Kreye, The cold spray process and its potential for industrial applications, J. Therm. Spray Technol. 15 (2006) 223-232.

[7] T. Schmidt, F. Gärtner, H. Assadi, H. Kreye, Development of a generalized parameter window for cold spray deposition, Acta Mater. 54 (2006) 729-742.

[8] E. Irissou, J.-G. Legoux, A. Ryabinin, B. Jodoin, C. Moreau, Review on cold spray process and technology: Part I - Intellectual property, J. Therm. Spray Technol. 17 (2008) 495-516.

[9] M. Fukumoto, H. Wada, K. Tanabe, M. Yamada, E. Yamaguchi, A. Niwa, M. Sugimoto, M. Izawa, Effect of substrate temperature on deposition behavior of copper particles on substrate surfaces in the cold spray process, J. Therm. Spray Technol. 16 (2007) 643-650.

[10] J. G. Legoux, E. Irissou, C. Moreau, Effect of substrate temperature on the formation mechanism of cold-sprayed aluminum, zinc, and tin coatings, J. Therm. Spray Technol. 16 (2007) 619-626.

[11] M. Kulmala, P. Vuoristo, Influence of process conditions in laser-assisted low-pressure cold spraying, Surf. Coat. Technol. 202 (2008) 4503-4508.

[12] Y. Danlos, S. Costil, X. Guo, H. Liao, C. Coddet, Ablation laser and heating laser combined to cold spraying, Surf. Coat. Technol. 205 (2010) 1055-1059.

[13] R. Lupoi, M. Sparkes, A. Cockburn, W. O'Neill, High speed titanium coatings by supersonic laser deposition, Mater. Letters 65 (2011) 3205-3207.

[14] S. Yin, X. Wang, W. Li, X. Guo, Examination on substrate preheating process in cold gas dynamic spraying, J. Therm. Spray Technol. 20 (2011) 852-859.

[15] V. Kosarev, S. Klinkov, A. Alkhimov, A. Papyrin, On some aspects of gas dynamics of the cold spray process, J. Therm. Spray Technol. 12 (2003) 265-281.

[16] I. Belov, I. Ginzburg, L. Shub, Supersonic underexpanded jet impingement upon flat plate, Int. J. Heat Mass Transfer 16 (1973) 2067-2076.

[17] C. Lee, M. Chung, K. Lim, Y. Kang, Measurement of heat transfer from a supersonic impinging jet onto an inclined flat plate at 45 deg, J. Heat Transfer 113 (1991) 769-772.

[18] M. Rahimi, I. Owen, J. Mistry, Impingement heat transfer in an under-expanded axisymmetric air jet, Int. J. Heat Mass Transfer 46 (2003) 263-272.

[19] V. Ramanujachari, S. Vijaykant, R. Roy, P. Ghanegaonkar, Heat transfer due to supersonic flow impingement on a vertical plate, Int. J. Heat Mass Transfer 48 (2005) 3707-3712.

[20] M. Limaye, R. Vedula, S. Prabhu, Local heat transfer distribution on a flat plate impinged by a compressible round air jet, Int. J. Therm. Sci. 49 (2010) 2157-2168.

[21] Y. Chung, K. Luo, N. Sandham, Numerical study of momentum and heat transfer in unsteady impinging jets, Int. J. Heat Fluid Flow 23 (2002) 592-600.

[22] H. Yoshida, K. Suenaga, R. Echigo, Turbulence structure and heat transfer of a two-dimensional impinging jet with gas-solid suspensions, Int. J. Heat Mass Transfer 33 (1990) 859-867.

[23] T. Yokomine, A. Shimizu, A. Saitoh, K. Higa, Heat transfer of multiple impinging jets with gas-solid suspensions, Exp. Therm. Fluid Sci. 26 (2002) 617-626.

[24] L. Jiji, Heat Conduction, second ed., Begell House, New York, 2003.

[25] A. Shapiro, The Dynamics and Thermodynamics of Compressible Fluid Flow, Volume II, The Ronald Press Company, New York, 1954.

[26] L. Jiji, Heat Convection, Springer-Verlag, Netherlands, 2006.

8. LIST OF FIGURES

lick here to download high resolution image

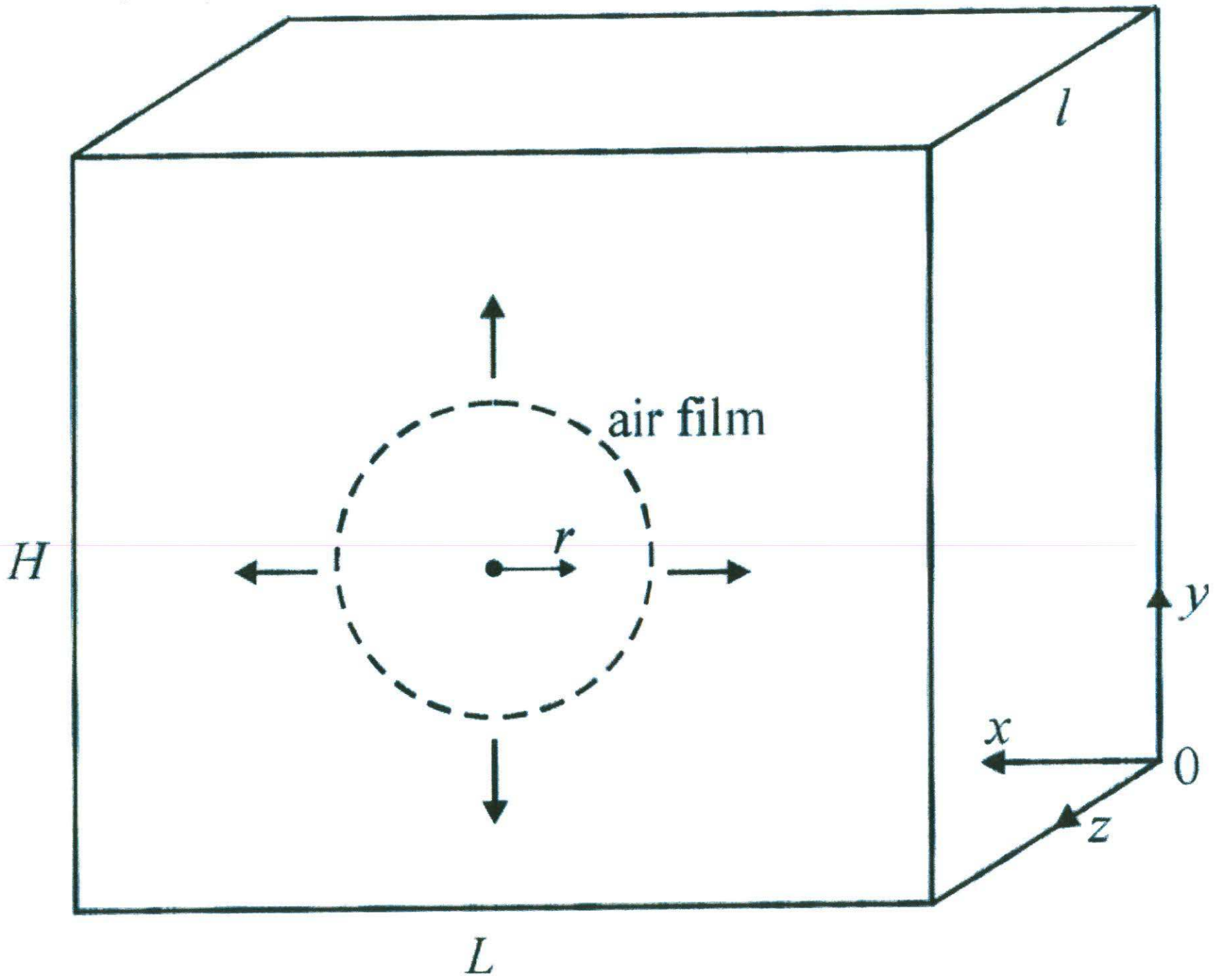

lick here to download high resolution image

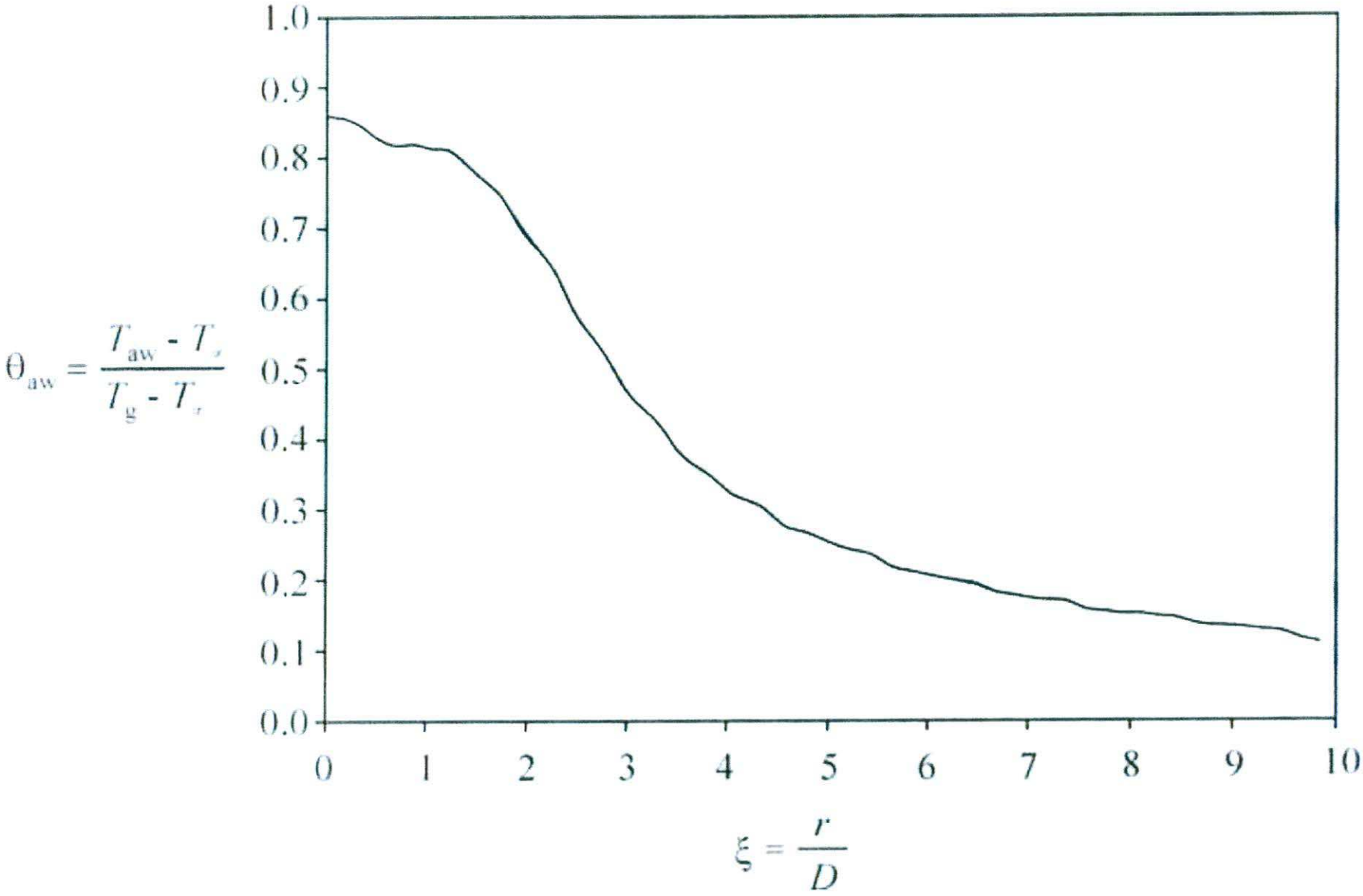

lick here to download high resolution image

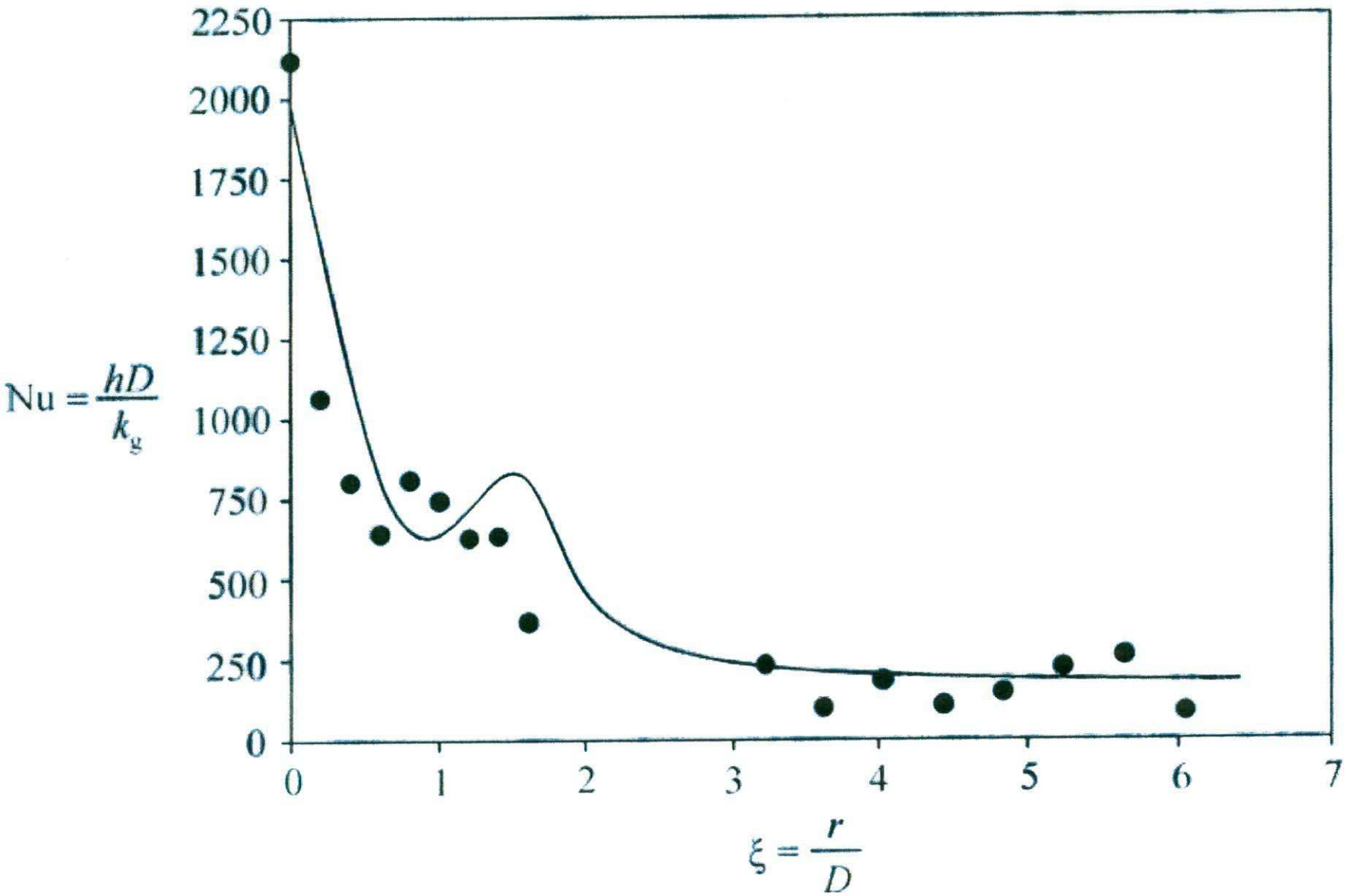

lick here to download high resolution image

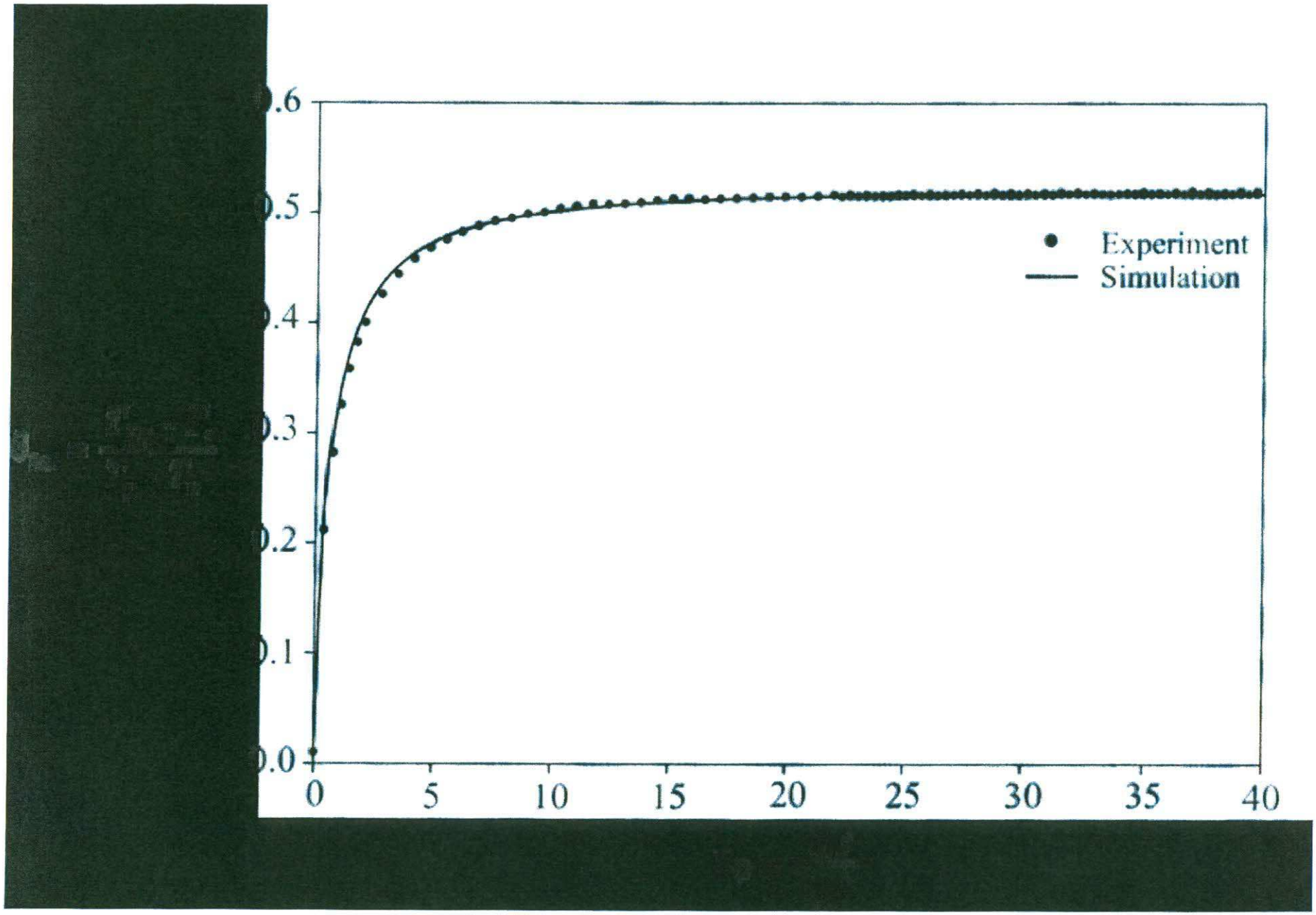

lick here to download high resolution image

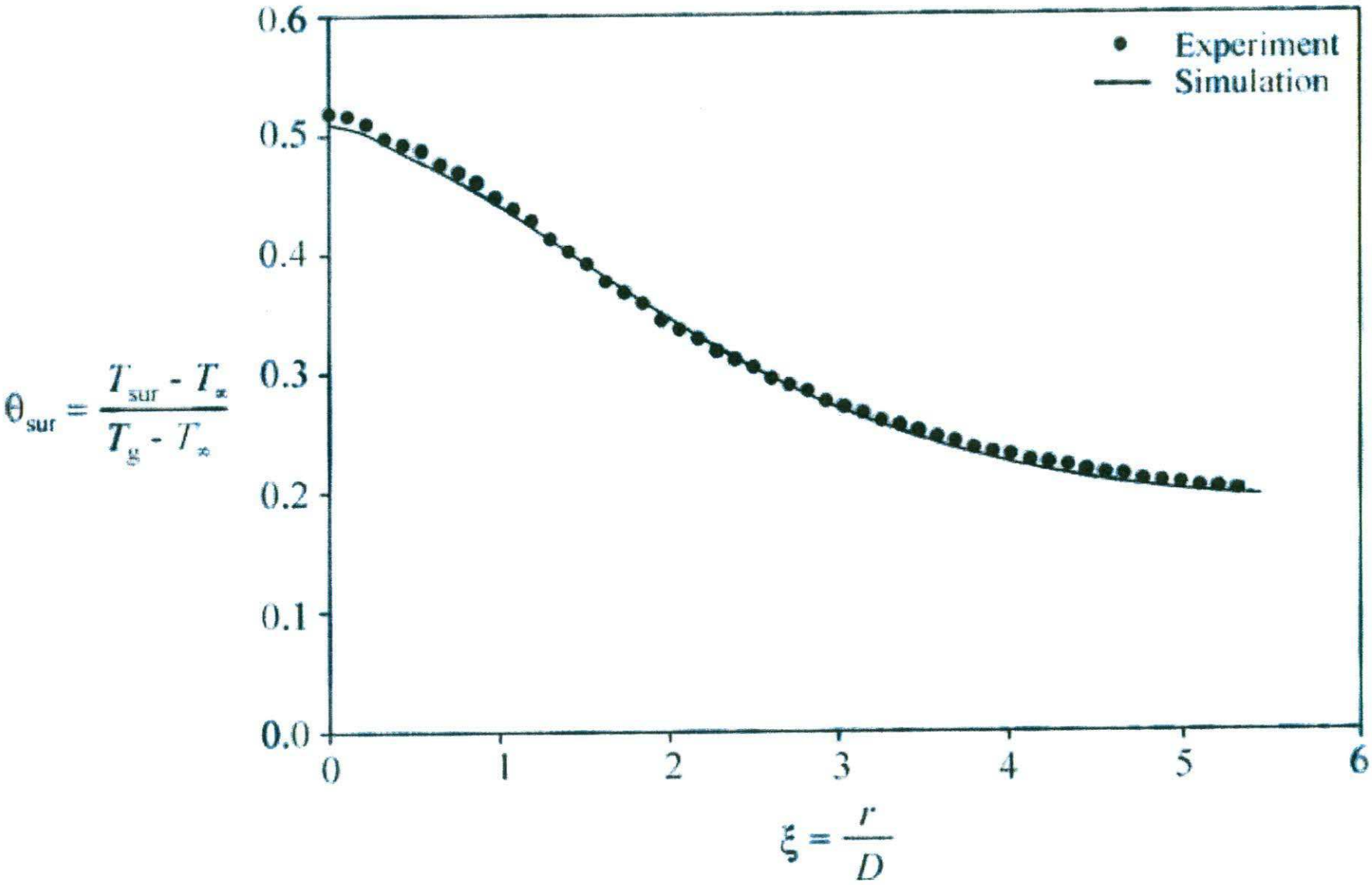

lick here to download high resolution image

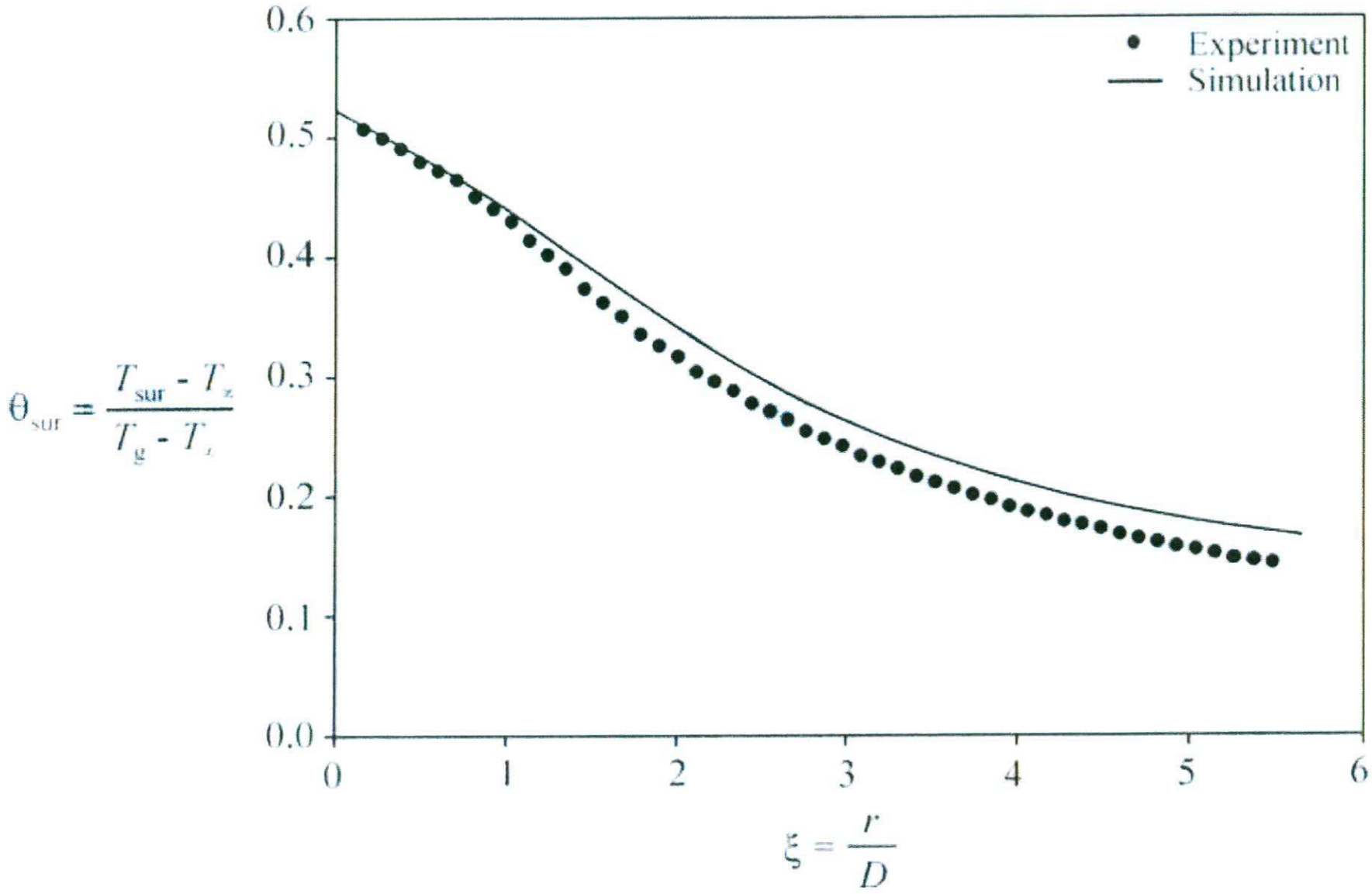

lick here to download high resolution image

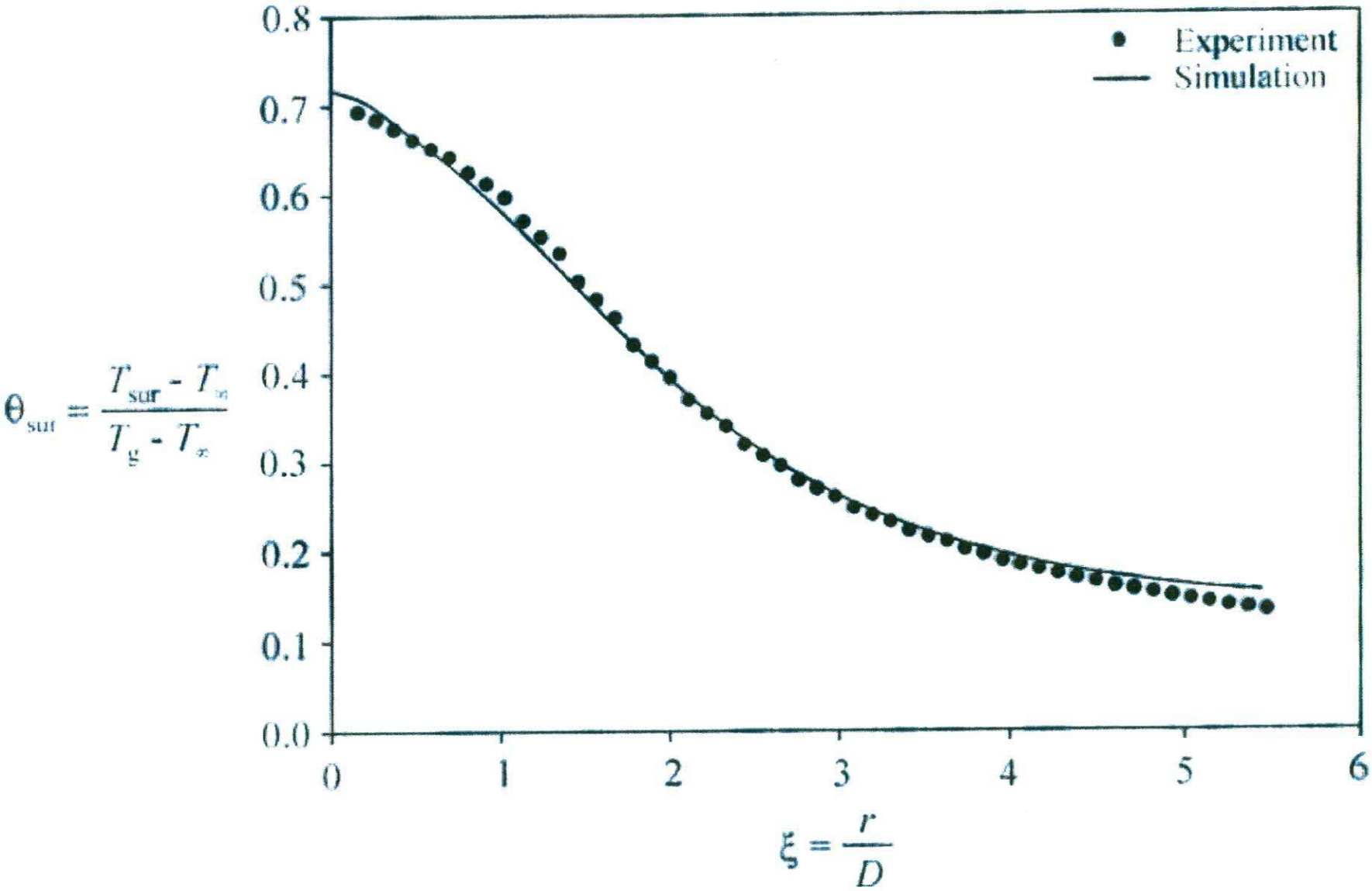

lick here to download high resolution image

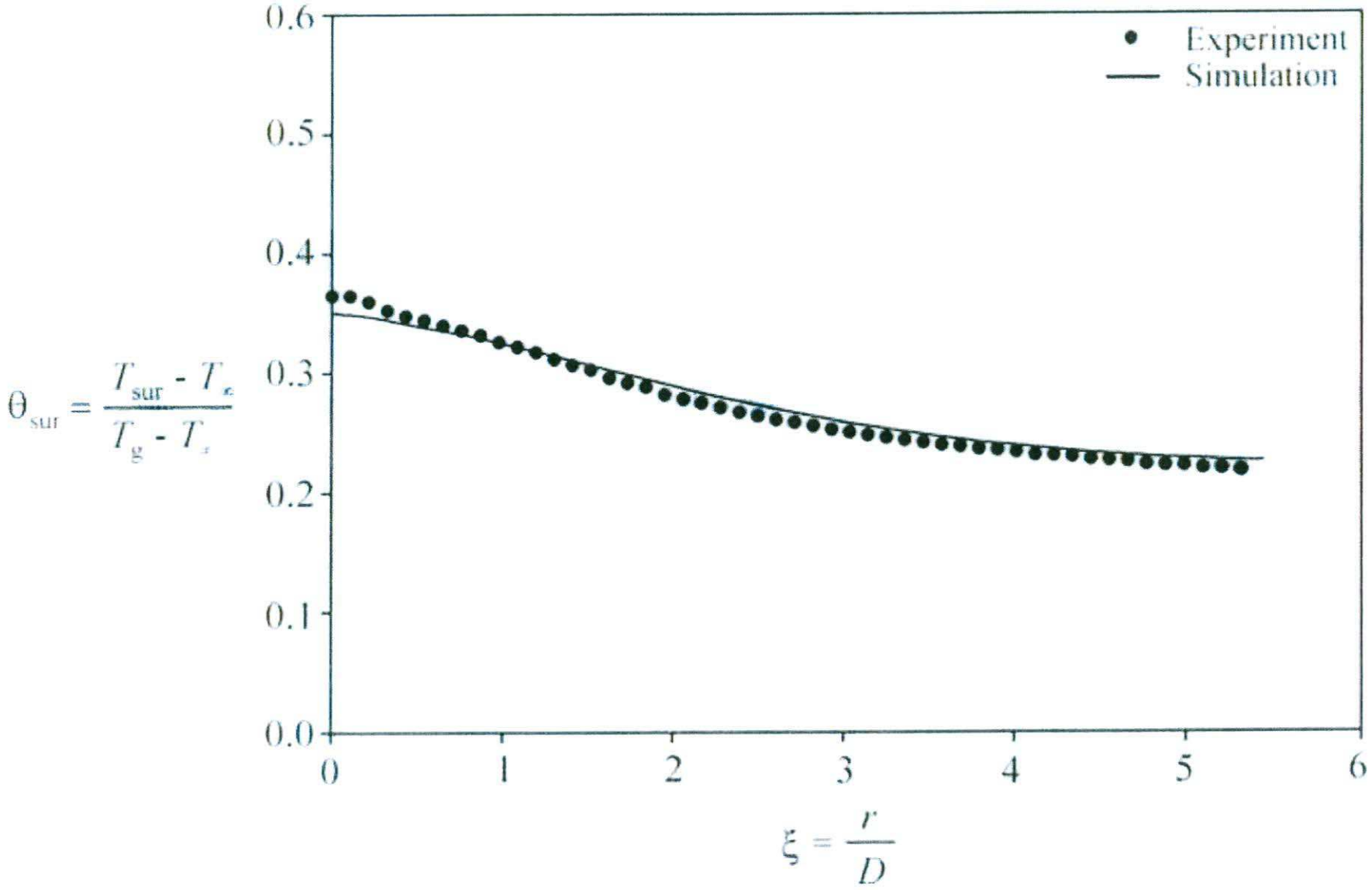

lick here to download high resolution image